

## Peculiar electronic, strong in-plane and out-of-plane second harmonic generation and piezoelectric properties of atomic-thick $\alpha\text{-M}_2\text{X}_3$ ( $\text{M}=\text{Ga, In}$ ; $\text{X}=\text{S, Se}$ ): role of spontaneous electric dipole orientations

Supplementary information

Lei Hu\*, Xuri Huang\*

*Institute of Theoretical Chemistry, Jilin University, Changchun 130000, People's Republic of China*

\*To whom correspondence should be addressed. Email: [598450225@qq.com](mailto:598450225@qq.com); [Xurihuang12@gmail.com](mailto:Xurihuang12@gmail.com)

**SI-1** The SHG properties of 2D materials are very sensitive to bandgaps. For instance, the SHG coefficient is reduced by 25% when the conduction bands are only shifted up by 0.19 eV for monolayer MoS<sub>2</sub>.<sup>1</sup> Herein, we tune the fraction of exact exchange (EE) of the HSE06 functional to achieve accurate bandgaps. We find the bandgap calculation with 30% EE generates a bandgap of 1.48 eV for  $\alpha\text{-M}_2\text{X}_3$  bulk crystals, in good agreement with its experimental bandgap of 1.42 eV.<sup>2</sup> Moreover, another calculation using HSE06 with 15% EE attained an indirect bandgap of 1.09 eV being nearly identical to the experimental bandgap of 1.10 eV for bulk MoSe<sub>2</sub>.<sup>3</sup> We thereby use HSE06 incorporating 30% EE to obtain the accurate bandgaps of single- and few-layer  $\alpha\text{-M}_2\text{X}_3$ . It should be noted bandgap calculations with larger EE fraction generate wider bandgaps.

**SI-2** The SHG coefficients are calculated using the length gauge formulism at the independent-particle level derived by Aversa and Sipe<sup>4</sup> and rearranged by Rashkeev et al.<sup>5</sup> The static SHG coefficients is given as the following equation

$$\begin{aligned}\chi_{abc}^{(2)}(-2\omega, \omega, \omega) &= \chi_{abc}^e(-2\omega, \omega, \omega) + \chi_{abc}^i(-2\omega, \omega, \omega) \\ &= \frac{e^3}{h^2 V} \sum_{nml,k} \frac{r_{nm}^a \{ r_{ml}^b r_{ln}^c \}}{\omega_{nm} \omega_{ml} \omega_{ln}} [\omega_n f_{ml} + \omega_m f_{ln} + \omega_l f_{nm}] \\ &\quad + \frac{ie^3}{4h^2 V} \sum_{nml,k} \frac{f_{nm}}{\omega_{nm}^2} [r_{nm}^a (r_{mn;c}^b + r_{mn;b}^c)]\end{aligned}$$

$$+r_{nm}^b(r_{mn;c}^a+r_{mn;a}^c)+r_{nm}^c(r_{mn;b}^a+r_{mn;a}^b)] . [1]$$

The dynamic SHG coefficients is expressed as

$$\begin{aligned} \chi_{abc}^e(-2\omega, \omega, \omega) = & \frac{e^3}{h^2 V} \sum_{nml,k} \frac{r_{nm}^a \{ r_{ml}^b r_{ln}^c \}}{\omega_{ln} - \omega_{ml}} \left[ \frac{2f_{mn}}{\omega_{mn} - 2\omega} + \frac{f_{ln}}{\omega_{ln} - \omega} + \frac{f_{ml}}{\omega_{ml} - \omega} \right] \\ & + \frac{i}{2} \frac{e^3}{h^2 V} \sum_{nm,k} f_{mn} \left[ \frac{2}{\omega_{mn} (\omega_{mn} - 2\omega)} r_{nm}^a (r_{nm;c}^b + r_{nm;b}^c) \right. \\ & + \frac{1}{\omega_{mn} (\omega_{mn} - 2\omega)} (r_{nm}^b r_{nm;c}^a + r_{nm}^c r_{nm;b}^a) \\ & + \frac{1}{\omega_{mn}^2} \left( \frac{1}{\omega_{mn} - \omega} - \frac{4}{\omega_{mn} - 2\omega} \right) r_{nm}^a (r_{nm}^b \Delta_{mn}^c + r_{mn}^c \Delta_{mn}^b) \\ & \left. - \frac{1}{2\omega_{mn} (\omega_{mn} - \omega)} \times (r_{nm;a}^b r_{nm}^c + r_{nm;a}^c r_{nm}^b) \right] . \quad [2] \end{aligned}$$

Because a vacuum space of more than 20 Å is added, the unit cell volume  $V$  in Eqn. [1] and [2] should be in place of the effective unit cell volume  $V_{eff}$  when calculating SHG coefficients. For monolayers and few-layers, the effective volume is simply obtained by multiplying the area of in-plane unit cell and the effective thickness. The scissors correction is used to account for the bandgap underestimation in DFT-GGA calculations.

**SI-3** We establish a classic model to interpret the electric field in bilayer AA  $\alpha$ -M<sub>2</sub>X<sub>3</sub> is much stronger than that in AB  $\alpha$ -M<sub>2</sub>X<sub>3</sub>. The  $\alpha$ -M<sub>2</sub>X<sub>3</sub> layer is considered as an electric dipole, where the minus sign (−) represents the center of negative charges ( $X^{2-}$ ) and the positive sign (+) denotes the center of positive charges ( $M^{3+}$ ). In AA  $\alpha$ -M<sub>2</sub>X<sub>3</sub>, the positive charge center of the top layer is neighbored by the negative charge center from the bottom layer, as shown in Fig. S1, which results in a strong electric field according to the classical electrodynamics. In AB  $\alpha$ -M<sub>2</sub>X<sub>3</sub>, the positive charge center from the top layer is neighbored by another positive charge center from the bottom layer, resulting in a void space with zero electric field. Moreover, the negative charge center of the top layer in AA and AB is less affected by the charges from the bottom layer. In brief, we have demonstrated the electric field of AB is significantly reduced compared with that in AA.

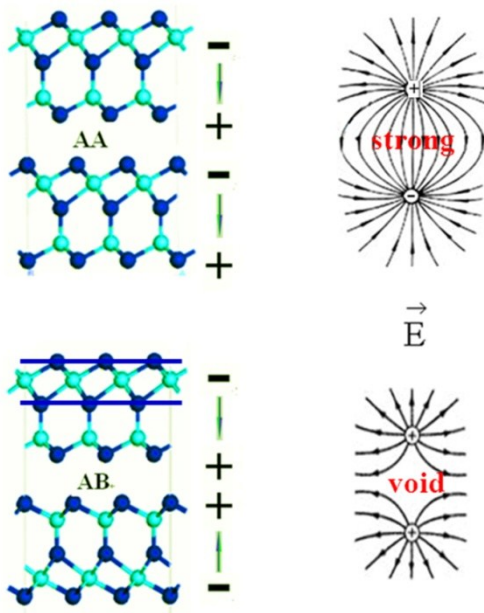


**Fig.S1** The electric field  $\vec{E}$  of bilayer AA and AB  $\alpha\text{-M}_2\text{X}_3$ . The green and blue atoms respectively denote M (M=Ga, In) and X (X=S,Se) atoms. The two transverse lines indicate that the X atoms at the top of single-layer  $\alpha\text{-M}_2\text{X}_3$  are close in the vertical direction. Therefore, the top of single-layer  $\alpha\text{-M}_2\text{X}_3$  can be represented by the negative sign (−), while the bottom is represented by the positive sign (+).

#### SI-4

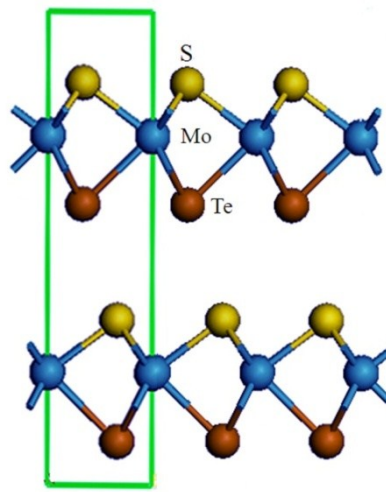


**Fig.S2** Schematics of bulk MoSTe composed of two MoSTe layers.

To highlight the significance of the piezoelectricity in AA  $\alpha\text{-M}_2\text{X}_3$ , we calculate the elastic and piezoelectric properties of bilayer MoSTe exfoliated from MoSTe bulk crystals (cf. Fig. S2) as a

recent calculation finds multilayer MoSTe (b) has large piezoelectric coefficients  $d_{33}$  of 13.517 pm/V and  $d_{31}$  of -1.234 pm/V.<sup>6</sup> As shown in Table S1, the elastic constant of bilayer MoSTe is twice that of monolayer MoSTe ( $C_{11}=112.7$  N/m,  $C_{12}=22.7$  N/m).<sup>6</sup> This is because, of the same strain, the force needed for bilayers is twice that of monolayers. Similar to MoSTe bulk crystals, the  $e_{11}$  ( $d_{11}$ ) coefficient of bilayers vanishes. Remarkably, the large  $d_{33}$  coefficient in multilayer MoSTe vanishes in the atomic-thick bilayer, and the large  $d_{31}$  coefficient decreases to -0.417 pm/V in the bilayer.

**Table S1** calculated elastic constants  $C_{ij}$  (N/m) and piezoelectric coefficients  $e_{ij}$  ( $10^{-10}$  C/m) and  $d_{ij}$  (pm/V) of bilayer MoSTe.

structure	$C_{11}$	$C_{12}$	$e_{11}$	$d_{11}$	$e_{31}$	$e_{31}$
bilayer	223.3	53.2	0	0	-1.15	-0.417

Additionally, we list the POSCAR file of bilayer MoSTe exploited from the above bulk crystal to facilitate readers to reproduce its elastic and piezoelectric coefficients in VASP calculations.

### MoSTe bilayer

```

1.000000000000000
2.9122510401769959 -1.6813889219939513 0.000000000000000
0.000000000000000 3.3627778439879026 0.000000000000000
0.000000000000000 0.000000000000000 35.000000000000000
S Mo Te
2 2 2

```

### Direct

```

0.666666666666643 0.333333333333357 0.3147745015930269
0.333333333333357 0.666666666666643 0.1255843281539999
0.000000000000000 0.000000000000000 0.0835675259508278
0.000000000000000 0.000000000000000 0.2727114154456826
0.666666666666643 0.333333333333357 0.2182171940206690

```

0.333333333333357 0.666666666666643 0.0290627327479865

**SI-5** To facilitate readers to reproduce the electronic, SHG and piezoelectric properties of bilayer AA and AB  $\alpha$ -Ga<sub>2</sub>S<sub>3</sub>, we supply their POSCAR file.

**bilayerAAGa<sub>2</sub>S<sub>3</sub>**

1.000000000000000  
3.1125811495302553 -1.7970495645558429 0.000000000000000  
0.000000000000000 3.5940991291116817 0.000000000000000  
0.000000000000000 0.000000000000000 42.000000000000000

S Ga  
6 4

Direct

0.000000000000000 0.000000000000000 0.1658998020407410  
0.000000000000000 0.000000000000000 0.0240956460959655  
0.666666666666643 0.333333333333357 0.3812008250631944  
0.6666666666666714 0.333333333333357 0.2393988489353072  
0.6666666666666714 0.333333333333357 0.1017331858221226  
0.333333333333357 0.666666666666643 0.3169297367611112  
0.000000000000000 0.000000000000000 0.3535717759510197  
0.666666666666643 0.333333333333357 0.0494509075966795  
0.333333333333357 0.666666666666643 0.2646385323618680  
0.333333333333357 0.666666666666643 0.1383546679434185

**bilayerABGa<sub>2</sub>S<sub>3</sub>**

1.000000000000000  
3.1121792839657227 -1.7968175473639860 0.000000000000000  
0.000000000000000 3.5936350947279712 0.000000000000000  
0.000000000000000 0.000000000000000 42.000000000000000

S Ga  
6 4

Direct

0.000000000000000 0.000000000000000 0.2314952026941349  
0.000000000000000 0.000000000000000 0.3734108800042285  
0.6666669999999968 0.3333330000000032 0.5898281865015894  
0.6666669999999968 0.3333330000000032 0.4479634724971330  
0.6666669999999968 0.3333330000000032 0.2958194235699879  
0.3333329999999961 0.6666699999999968 0.5255283473883566  
0.000000000000000 0.000000000000000 0.5622662440271677  
0.6666669999999968 0.3333330000000032 0.3480737631479691

0.333330000000032 0.666669999999968 0.4732852440044870  
0.3333329999999961 0.666669999999968 0.2590592361649235

## References

1. C. Y. Wang and G. Y. Guo, *J. Phys. Chem. C*, 2015, **119**, 13268.
2. Y. Watanabe, S. Kaneko, H. Kawazoe and M. Yamane, *Phys. Rev. B: Condens.Matter.Phys.*, 1989, **40**, 3133.
3. H. Mirhosseini, G. Roma, J. Kiss and C. Felser, *Phys. Rev. B: Condens.Matter.Phys.*, 2014, **89**, 205301.
4. C. Aversa and J. E. Sipe, *Phys.Rev. B: Condens.Matter.Phys.*, 1995, **52**, 14636.
5. S. N. Rashkeev , W. R. L. Lambrecht and B. Segall, *Phys.Rev. B: Condens.Matter.Phys.*, 1998, **57**, 3905.
6. L. Dong, J. Lou and V. B. Shenoy, *ACS Nano*, 2017, **11**, 8242.